UCRL 8328

UNIVERSITY OF CALIFORNIA

Radiation Laboratory

BERKELEY, CALIFORNIA

DISCLAIMER

UCRL-8328

UNIVERSITY OF CALIFORNIA

Radiation Laboratory
Berkeley, California

Contract No. W-7405-eng-48

A HYDROMAGNETIC CAPACITOR

Oscar Anderson, William R. Baker, Alexander Bratenahl,
Harold P. Furth, and Wulf B. Kunkel

June 23, 1958

Printed for the U. S. Atomic Energy Commission

A HYDROMAGNETIC CAPACITOR

Oscar Anderson, William R. Baker, Alexander Bratenahl,
Harold P. Furth, and Wulf B. Kunkel

Radiation Laboratory
University of California
Berkeley, California

June 23, 1958

ABSTRACT

Very high dielectric constants can easily be achieved by means of an ionized gas in a strong magnetic field. When an orthogonal electric field is applied, the resultant particle drift stores electrical energy. In a coaxial capacitor, which makes use of a rotating plasma disk, dielectric constants in the range 10^6 to 10^8 have been measured. The potential usefulness of hydromagnetic capacitors in fast-discharge work is considered.

A HYDROMAGNETIC CAPACITOR*

Oscar Anderson,† William R. Baker,† Alexander Bratenahl,† Harold P. Furth,§ and Wulf B. Kunkel†

Radiation Laboratory
University of California
Berkeley, California

June 23, 1958

INTRODUCTION

For many research purposes[1,2] it has been found desirable to create large and sudden concentrations of electromagnetic energy by means of fast capacitors. In some experiments an energy density u_m of as much as 4000 joules/cm^3 is reached, corresponding to a magnetic field of $B = 10^6$ gauss:

$$u_m = B^2/8\pi = p_m.^{**} \qquad (1)$$

The associated magnetic pressure p_m equals 5.6×10^5 psi., which is just on the border line of the strength of materials.

It is instructive to contrast the high feasible values of u_m with the highest values of the electrostatic energy density u_e that can readily be achieved over large volumes. As is well known, electric field strengths are severely limited by the danger of electrical breakdown. Taking a marginal value of $E = 5 \times 10^5$ volts/cm, one obtains an energy density $u_e = K \times 10^{-2}$ joules/cm^3, where

$$u_e = K\ E^2/8\pi \qquad (2)$$

and K is the dielectric constant.

Suppose that K is comparable to unity. It follows that a capacitor-powered experiment conducted at the 10^6-gauss level must be surrounded by a capacitor volume several million times as large as the active experimental volume. Such a bulky arrangement is often inconvenient, and imposes inherent limitations on the discharge time, as is seen in a later section.

---

*Work done under the auspices of the U. S. Atomic Energy Commission.

†University of California Radiation Laboratory, Berkeley, California

§University of California Radiation Laboratory, Livermore, California.

**Gaussian units are used throughout this paper.

Suppose, however, that a dielectric constant of a few million can be achieved; then the density of capacitative energy storage can be made just as high as the maximum energy density desired in most experiments. It follows that the physical dimensions of source and of load can be made comparable, with a corresponding advantage in the attainable discharge time.

Conventional capacitor materials fall far short of satisfying the condition $K = 10^6$. A popular choice of dielectric for fast-discharge work is distilled water, for which K is about 100. Materials such as barium titanate approach $K = 10^4$, but in this material the maximum permissible E is limited in practice to about 5×10^4 volts/cm. There does exist, however, a conventional capacitive device that readily simulates dielectric constants as high as 10^{15}, and that is the homopolar generator.

It is well known that rotating equipment is far superior to ordinary capacitor banks when it comes to storing high electrical energy densities. An expression for the effective dielectric constant of a rotating ring of conductive material can be derived as follows. In the state of rotational equilibrium the radial electric field induced by motion at velocity v_θ through the axial magnetic field B_z just balances the applied electric field E_r. Therefore we have the simple relationship

$$v_\theta B_z / c = E_r , \tag{3}$$

where c is the speed of light in vacuum. The effective dielectric constant K is now defined by the equation

$$K(E_r^2 / 8\pi) = E_r^2 / 8\pi + \tfrac{1}{2} \rho \, v_\theta^2 / 2 . \tag{4}$$

It follows:

$$K = 1 + 4\pi\rho c^2 / B_z^2 , \tag{5}$$

which is bound to be a very large number when ρ is taken as the mass density of a solid material.

The usefulness of ordinary rotating machinery in fast-discharge work is limited precisely by the fact that K cannot be kept to moderate values, such as a few million. Since the velocity of electromagnetic waves in a dielectric is given by

$$v_w = c / \sqrt{K} , \tag{6}$$

the short-circuit discharge time of a 2-cm-long coaxial capacitor (Fig. 2b) with $K = 10^{15}$, for instance, will amount to about 10^{-3} sec. Most experiments at high energy density that are of interest at present, being of moderate physical size, require energy input times very much shorter than 10^{-3} sec. Making the rotating system much smaller than a few centimeters--which seems possible because of the tremendous attainable energy density--is physically inconvenient and is not much help when such extremely short times as 10^{-7} or 10^{-8} sec are desired. Moreover, another and often more serious limitation of rigid rotors lies in the fact that the maximum peripheral speed of solid conductors is only of the order of 10^5 cm/sec. This means that ordinary homopolar generators are limited to low voltages.

We have therefore been interested in developing a homopolar generator with an effective dielectric constant in the vicinity of 10^6 rather than 10^{15}. In this case the discharge time of a 2-cm-long unit could ideally be brought down into the range of 10^{-7} to 10^{-8} sec. In other words, we have been looking for a conducting flywheel of very low inertia. The mass density of the material needed for the rotor of such a homopolar generator is about 10^{-9} times the density of copper. As will be seen below, a low-density fully ionized gas meets this requirement rather conveniently. Moreover, in such a medium the velocity can be made much larger than in a spinning solid, so that electric fields of the order of 10^3 volts/cm can be supported by magnetic fields of only a few kilogauss.

PLASMA AS A DIELECTRIC MATERIAL

When orthogonal electric and magnetic fields are applied to an ionized gas, there results a drift motion of both ions and electrons in the same direction (Fig. 1). This neutral drift is analogous to the equilibrium motion of the homopolar rotor. In the process of assuming their equilibrium drift motion, the plasma particles undergo a finite mean displacement, in the direction of the electric field. This displacement is opposite for particles of opposite charge. The precise shape of each particle trajectory depends on whether the electric field rises slowly or rapidly compared with the cyclotron period. In Fig. 1, as in most of this analysis, effects due to the finite duration of the cyclotron period are neglected. Furthermore, the Larmor radius is always considered small compared with the radius of the drift rotation. These two approximations are valid in most practical situations.

The finite opposite displacement of positive and negative plasma particles is reminiscent of the behavior of an ordinary dielectric medium when an electric field is applied. The analogy is, however, better seen in a description of macroscopic behavior. The equation of motion of a volume element of plasma is given by

$$\rho \frac{d\vec{v}}{dt} = \frac{\vec{j} \times \vec{B}}{c} - g\vec{v}, \tag{7}$$

where $\vec{v}$ is the plasma velocity, $\vec{j}$ the plasma current density, and $g\vec{v}$ denotes viscous drag. The scalar function g varies in time and space in a manner determined by the boundary conditions on the plasma. Since the Larmor motion is being neglected, we have at all times the approximate relationship

$$\vec{v} = c \frac{\vec{E} \times \vec{B}}{B^2}, \tag{8}$$

of which Eq. (3) is a particular case. (In Eq. (8), the quantity $\vec{E}$ is actually the applied electric field minus a correction term $\eta\vec{j} + \Delta\vec{E}$, where η is the plasma resistivity and $\Delta\vec{E}$ takes into account any possible electrode sheath effect.) The current density supported by the displacement of plasma particles is orthogonal to $\vec{B}$ and therefore can be written as

$$\vec{j} = \frac{\rho c}{B^2} \vec{B} \times \frac{d\vec{v}}{dt} + \frac{gc}{B^2} \vec{B} \times \vec{v} = \frac{\rho c^2}{B^2} \frac{d\vec{E}}{dt} + \frac{gc^2}{B^2} \vec{E}. \tag{9}$$

Aside from the term in g, this is just the equation[3] for a polarizable medium having a dielectric constant K that is, as expected, identical with the K defined by Eq. (5). The effect of the viscosity term $(gc^2/B^2)\vec{E}$ is to provide for a leakage current density through the dielectric medium.

There are, of course important differences between a rotating plasma and an ordinary dielectric medium. For instance, in the plasma, just as in a solid homopolar generator, the "energy of polarization" resides in the kinetic energy of particle drift rather than in the potential energy of stretched molecular bonds or oriented molecular dipoles. A second difference, related to the first, is that in the plasma the charged particles (in a solid homopolar generator, the electrons) undergo a macroscopic displacement rather than one on only a molecular scale; therefore it is better to regard the current as a true current rather than as a mere

displacement current. If the electrodes are not good sources and sinks of ions and electrons, discontinuities tend to occur there. In particular, the lack of free ions at the anode may cause a sharp local voltage drop to appear there that dominates the electrical behavior.[4] For reasons that are not yet completely understood, electrode drops have not interfered with the experiments reported here. It seems possible that collisions are capable of preventing the formation of excessive electrode sheaths when the gas density is sufficiently high.

The basic resemblance of rotating and capacitor-type electrical equipment was noted earlier. It is easy to see that a homopolar generator using a body of plasma as its rotor (Fig. 2a) will resemble a coaxial capacitor (Fig. 2b) in considerable detail. The acceleration of an element of plasma may be written, by Eq. (7), as

$$\rho(dv_\theta/dt) = j_r B_z/c, \tag{10}$$

where the viscosity term has been neglected. The radial current density j_r is related to the total radial current I by the equation

$$I = 2\pi\, r\ell j_r, \tag{11}$$

where ℓ is the thickness of the plasma disk. If B_z is uniform, then dv_θ/dt will vary inversely as the distance r from the axis of rotation. Therefore, v_θ will also be distributed as $1/r$. From Eq. (3) it then follows that E_r varies as $1/r$. This means that the distribution of the electric field inside the plasma disk is like that of the electric field inside a coaxial capacitor, and unlike that of the electric field inside a rigid homopolar rotor, where v_θ varies as r. It is interesting to note, incidentally, that the r and $1/r$ velocity distributions of a rotating fluid are unique in that they tend to maintain themselves in the presence of internal viscous drag.

From Eqs. (10) and (11) it follows that the total angular momentum P_θ imparted to the plasma is given by

$$P_\theta = (B_z/c) \int I\,dt \int r\,dr \tag{12}$$

$$= (1/2\pi c)\, B_z A Q, \tag{13}$$

where Q is the total charge passed during acceleration and A is the area

of the rotating plasma disk. The relationship between rotational kinetic energy and "electrical" energy storage in a rotor has already been discussed in connection with Eq. (5). It is not surprising that the two quantities $Q = C\,V$ and $U = \frac{1}{2} CV^2$, which characterize a capacitor, correspond closely to angular momentum and kinetic energy, the two constants of the motion for a spinning plasma.

EXPERIMENTAL RESULTS

The basic theoretical features of the hydromagnetic capacitor have been documented experimentally by means of a small flat discharge chamber, shown in Fig. 2a. This device is placed between the poles of an 18,000-gauss dc electromagnet.* A radial electric field is then applied between the two concentric electrodes, which are respectively 3 in. and 9-3/4 in. in diameter. The discharge chamber is insulated at its top and bottom by two Vicor disks, spaced 5/8 in. apart. The vacuum capacity of the device, seen as a coaxial capacitor, is therefore about 0.75 μμf.

A variety of gases from hydrogen to iodine vapor have been used to carry the discharge, but most of the work was done with argon in the 25- to 500-micron pressure range. Satisfactory operation could be achieved with a 48-μf source capacitor bank at 5 to 8 kv initial voltage.

In Fig. 3 are shown some typical oscilloscope traces of current and of voltage across the discharge. In the absence of any axial magnetic field, (top trace) the discharge acts simply like a short circuit. The current then oscillates with a characteristic period determined by the source capacity C_s and the source and load inductances L_s and L_h:

$$\tau_s \cong 2\pi\sqrt{C_s\,(L_s + L_h)}\,. \tag{14}$$

There is no capacitative reaction, because the null-magnetic-field case corresponds to having an infinite dielectric constant in the hydromagnetic capacitor. In the remainder of Fig. 3, the axial magnetic field is set at 13,000 gauss and the gas pressure is reduced in steps from 450 to 200 to 100 μ of argon. This corresponds to a theoretical variation of the dielectric constant from 7.3×10^7 to 3.2×10^7 to 1.6×10^7, or a variation in effective capacity from 55 to 24 to 12 μf.

---

*A similar configuration has been described by Early and Dow in connection with aerodynamic experiments.[5]

As the theoretical capacity of the hydromagnetic device is made smaller than the source capacity of 48 μf, a marked effect on the discharge pattern becomes noticeable. The effective capacity of the circuit,

$$C = C_s C_h/(C_s + C_h), \tag{15}$$

begins to approximate C_h instead of C_s, with a corresponding change in the ringing frequency of the circuit. Some theoretical curves computed for a two-capacitor circuit with series inductance $L = L_s + L_h$ and damping resistor $R = R_s + R_h$ are shown in Fig. 4. When the full capacitor C_s is discharged into the empty one C_h, the initial charge surges back and forth between the two capacitors until resistive damping brings them to their equilibrium voltage. If C_h/C_s is large, then the source capacitor will be nearly drained at equilibrium, and the equilibrium voltage will be low. Conversely, if C_h/C_s is small, the equilibrium voltage will be close to the initial voltage. These features are readily discerned in the experimental circuit responses of Fig. 3. In addition it is clear that after damping of the initial transient, the system does not approach a constant equilibrium voltage, but rather one that decays with fair rapidity. In other words, charge is being drained from both C_s and C_h by what amounts to a leakage resistance R_L. A simple equivalent circuit for the whole system is given in Fig. 5.

The observed circuit responses of Fig. 3 confirm in a general way the expected capacitive behavior of the rotating plasma machine. A more quantitative study of charge storage (which by Eq. (13) is the same as angular momentum storage) can be made by applying a direct short circuit to the device. This is done by the low-inductance "crowbar" circuit indicated on Fig. 5. As can be seen on the experimental traces of Fig. 6, when the crowbar circuit is fired, a fast transient oscillation does in fact occur. As expected, the short-circuit current out of the hydromagnetic capacitor starts in the opposite direction from the charging current. Because the short-circuit inductance $L_h + L_c$ is considerably smaller than the charging inductance $L_s + L_h$, the period of the short-circuit transient,

$$\tau_h = 2\pi\sqrt{C_h(L_h + L_c)}\,, \tag{16}$$

is much shorter than the period of the charging transient. The magnitude of the short-circuit current is correspondingly greater than that of the charging current. Thus even the present rather crude hydromagnetic device is a more powerful fast-discharge capacitor than its source capacitor bank, the volume of which is larger by a factor of 10^4.

By short-circuiting the hydromagnetic capacitor at various stages of its charging cycle, one can obtain an entire time-history of its effective capacity and its various dissipation mechanisms. The aggregate experimental results of two measurement series are given in Fig. 7a and b. Once the charging current has stopped, the effective capacity of the hydromagnetic device can be determined accurately from the voltage measured across the plasma at any time and the charge drawn out during the first quarter cycle of a subsequent crowbar transient. The capacity computed in this way has been found fairly constant for the first 5 to 10 μsec, but sometimes diminishes by a factor of two or more by the time the voltage has decayed to 1/e. Experimental values of effective dielectric constants agree well with theoretical values computed by Eq. (5) on the basis of the initial gas density in the discharge chamber. When axial magnetic field, plasma density, and gas type were varied widely, so as to give theoretical dielectric constants K_{th} ranging from 10^6 to 10^8, the ratio K_{ex}/K_{th} was found to lie consistently within the limits 1 and 2.

Aside from the effective capacity of the hydromagnetic device, its effective shunt resistance--that is to say, its "leakiness" as a capacitor--must be considered. As has been noted in connection with Eq. (9), the physical phenomenon that underlies the process of charge leakage is, of course, the impairment of free plasma rotation by viscosity. If there is viscous drag of the plasma against the surfaces of the discharge chamber, then a fraction of the accelerating current is wasted in balancing the viscous retarding torque. Viscosity is one of the many diffusion-type phenomena that occur in a plasma, and is connected, in particular, with ion velocity diffusion due to ion-ion collisions. It can be shown that the viscosity coefficient of a fully ionized gas is drastically reduced by the presence of a magnetic field if the collision frequency between ions is smaller than their cyclotron frequency.[6] It is useful here to speak of a velocity-diffusion distance s_v,

which gives the effective range of viscous damping forces. Like the ordinary plasma particle diffusion distance s_d, the quantity s_v increases in time as $\sqrt{t}$. Whether a system is seriously damped after a given interval of time depends on whether it is large or small compared with s_v, just as the question of actual plasma containment in a system depends on whether the system is large or small compared with s_d. The quantities s_v and s_d are generally of the same magnitude, and both vary inversely as the 3/4 power of the plasma temperature, if $\beta = p/B^2$ is kept constant. At any rate it should be possible to design a hydromagnetic capacitor filled with a fully ionized plasma of low atomic number that would for many practical purposes have negligible viscosity and plasma-diffusion troubles. This is particularly true, of course, if the plasma can be kept from making good contact with the end plates, partly by means of the pinch force associated with the charging current, and partly because of rotational effects, some of which are indicated in the next section. These axial-containment properties of the configuration are discussed in detail elsewhere.[7] Since ideal plasma conditions are not yet approached very closely in actual experiments, pronounced viscous drag against the walls of the discharge chamber is usually observed.

An example of rather serious charge leakage from the hydromagnetic capacitor when filled with argon is shown in Fig. 8. The total extractable charge A is graphed as a function of time for purposes of comparison with the total input current B and input charge C. Evidently, by the time of maximum charge storage, about twice as much charge has leaked through the system as has been stored in recoverable form. By differentiating the charge storage curve A, one obtains the true charging current D. The leakage current is then the difference between B and D. The voltages across the hydromagnetic capacitor E and source capacitor F are also shown. Note that the voltage curve E rises more rapidly than the charge curve A, thus demonstrating that the hydromagnetic capacitor has an effective series resistance as well as a shunt resistance. The series resistance, which represents the correction term omitted in Eq. (8), is relatively high in the early stages, possibly indicating the temporary existance of an anode sheath.

In order to obtain direct confirmation of the rather high theoretical velocities ascribed to the plasma homopolar rotor, a study was made of the Doppler shift of light from the rotating plasma. The spectrum of light coming tangentially from the outer rim of the rotor was photographed with the axial magnetic field first in one direction and then in the opposite direction. Figure 9 shows a typical result obtained with helium. The observed Doppler shifts have been of the expected magnitude, indicating peripheral velocities of the order of 5×10^6 cm/sec.

One of the most interesting experimental discoveries has been that the rotating plasma is apparently stable, even for conditions under which the energy density of rotation is comparable to the energy density of the axial magnetic field. From an elementary theoretical point of view one might have anticipated the familiar Helmholtz instability. The complete theory of stability is being investigated.

CENTRIFUGAL EFFECTS

When the plasma particles are moving with very high velocities, Eqs. (8) and (3) must be modified to take centrifugal force into account. The more general expression for azimuthal velocity is

$$v_\theta = (c/B_z)(E_r + mv_\theta^2/re) = c E_r/B_z + \Delta v_\theta . \qquad (17)$$

The size of the correction term depends essentially on the relative magnitude of the particle displacement in the electric field and the radius r from the axis of plasma rotation. For electrons the correction term is quite negligible, but for the ions the incremental velocity can actually be observed. The result is a diamagnetic effect. The slight relative velocity of ions and electrons gives rise to an azimuthal current density,

$$j_\theta = n_i e \Delta v_{\theta i} = n_i m_i v_\theta^2 c/B_z r , \qquad (18)$$

which is of just the right magnitude to balance the plasma centrifugal pressure by the Lorentz force

$$j_\theta B_z/c = \rho v_\theta^2/r. \qquad (19)$$

At high operating levels of the hydromagnetic capacitor, the azimuthal current causes a very noticeable bowing out of the lines of the axial magnetic field. One can also think of this effect as due to the outward

distention of the magnetic field when the centrifugal pressure of the plasma becomes comparable to the initial magnetic pressure. If this distortion is strong a considerable reduction of viscous drag at the end plates is expected, as mentioned in the preceding section. The resultant radial-field component can be detected by means of a pickup loop located near one of the Vicor end plates of the discharge chamber. A time-integrated signal from such a "spin loop" is shown in Fig. 10 together with other oscilloscope traces photographed simultaneously. Since the distortion of the magnetic field decays at about the same rate as the voltage signal, one can conclude that the rotating plasma is always contained by axial-magnetic-field pressure rather than by direct pressure against the outer electrode, as a neutral rotating gas would be. When the radial driving current is reversed, the spin loop signal retains its original direction, as expected.

It is interesting to consider what effect centrifugal distortion of the axial magnetic field has on the circuit response of the hydromagnetic capacitor. The capacity C_0 for the case of uniform particle density and B_0 is easily derived from the equations (neglecting the contribution from the vacuum field)

$$\tfrac{1}{2} C_0 V_0^2 = \pi \ell \int_{r_1}^{r_2} \rho_0 v_{\theta 0}^2 \, r dr, \tag{20}$$

$$V_0 = E_0 \, r \log \, r_2/r_1, \tag{21}$$

$$v_{\theta 0} = E_0/B_0 \, c. \tag{22}$$

Substituting Eqs. (21) and (22) into Eq. (20) one obtains

$$C_0 = (4\pi\rho_0 c^2/B_0^2) \, [\ell/2 \log (r_2/r_1)]. \tag{23}$$

To study the capacity for the case of centrifugally displaced density and B distributions, let us consider first the infinite-conductivity case. Then B assumes the same radial variation as ρ. Let this distribution be described by $\psi(r)$, with the normalization condition

$$\int_{r_1}^{r_2} \psi(r)\, r\,dr = \tfrac{1}{2}\,(r_2^2 - r_1^2). \tag{24}$$

The assumption of infinite conductivity implies

$$B/\rho = B_0/\rho_0 = \text{constant}. \tag{25}$$

It then follows from Eq. (10) that we have

$$v_\theta = (B_0/\rho_0)(Q/2\pi\ell)\,(1/r); \tag{26}$$

that is, v_θ has a $1/r$ variation just as in the uniform-density case. The total energy content can be written as

$$\tfrac{1}{2}\,C\,V^2 = Q^2/2C = \pi\ell \int_{r_1}^{r_2} \rho v_\theta^2\, r\,dr. \tag{27}$$

In accordance with Eq. (24), the mass density is given by

$$\rho = \rho_0 \psi(r), \tag{28}$$

and with Eqs. (23) and (26) one obtains finally

$$C = [C_0 \log (r_2/r_1)] \Big/ \int_{r_1}^{r_2} \psi\,(dr/r)\ . \tag{29}$$

In view of Eq. (24), this is conveniently written as

$$C = C_0\ \frac{2 \log \dfrac{r_2}{r_1}}{r_2^2 - r_1^2}\ \frac{\displaystyle\int_{r_1}^{r_2} \psi\, r\,dr}{\displaystyle\int_{r_1}^{r_2} \psi\ \frac{dr}{r}}\ . \tag{30}$$

The more ψ is peaked outward, the larger C must evidently become. In the limit $\psi \sim \delta(r - r_2)$ we obtain

$$C_\infty = C_0\ [2 \log (r_2/r_1)]/[1 - (r_1/r_2)^2]. \tag{31}$$

In the experimental case at hand, r_2/r_1 is about 3, so that we have

$$C_\infty = 2.45\ C_0.$$

The compatibility of this number with the experimental result $1 \leqslant K_{ex}/K_{th} \leqslant 2$ is interesting, but the experimental study of the correlation of K_{ex}/K_{th} with centrifugal distortion has not been carried out in sufficient detail for further analysis at present.

When the plasma of the hydromagnetic capacitor undergoes centrifugal displacement, its capacity is enlarged. Obviously there is now also some energy of deformation stored in the magnetic field. One may ask in what way this additional energy storage can be fitted into the circuit analysis. The answer is simply that, when the hydromagnetic capacitor is discharged, its capacity must return to normal, and the distended magnetic field expends its stored energy in accomplishing this capacity reduction. Let the energy stored be

$$U = Q^2/2C, \tag{32}$$

then one has

$$\frac{dU}{dt} = -\frac{1}{2}\ \frac{Q^2}{C^2}\ \frac{dC}{dt} + \frac{Q}{C}\ \frac{dQ}{dt}\ . \tag{33}$$

When C is reduced, the magnetic field clearly feeds positive energy into the circuit.

If one departs from the infinite-conductivity assumption, the calculation of capacity becomes somewhat more complicated, because the spatial distribution of ρ now differs from that of B. C slowly increases in time, thus dissipating capacitive energy, according to Eq. (33). (Meanwhile additional energy is being dissipated by viscosity, which acts to diminish Q.) When the device is crowbarred, an enlarged capacity is observed, as in the infinite-conductivity case, but less energy is now available. This is partly because rotational energy has been dissipated, partly because there is less deformation energy in the magnetic field, and partly because not all the rotational energy present can actually be drawn out. This last effect is similar to that which occurs in a string of capacitors if they carry unequal charges. After the resistive diffusion has proceeded so long that an appreciable amount of plasma is actually being lost from

the rotating system, the capacity decreases again. Since Q necessarily decreases at least at the same rate as C, capacity reduction now results in an energy loss, not a gain as was the case earlier.

THE USEFULNESS OF A CAPACITOR HAVING HIGH DIELECTRIC CONSTANT

The choice of electrical power source for an experiment is obviously governed by many considerations, some of which are highly technical. By way of illustration, it may be useful to note that the potentially cheapest and most powerful method of electrical energy storage is not capacitive at all, but inductive.[8] If one opens a current-carrying inductive circuit across a load impedance, magnetic energy from the storage inductance is transferred directly to the load. In this case, it is easy to make the electromagnetic energy density in the source comparable to that in the load. The reason for the relative unpopularity of inductive sources is to be found in the purely technical difficulty of interrupting a high-powered circuit.

The hydromagnetic capacitor permits energy storage at about the same energy density as a storage inductance, and is much easier to discharge into a load. The unit itself is relatively inexpensive and can be made to occupy a small fraction of the space required for conventional capacitors; however, auxiliary electrical equipment is needed to establish the magnetic field and set the plasma into rotation. The experiments performed to date do not furnish an adequate basis for technical comparisons between hydromagnetic and conventional capacitors. Relatively little is known about optimum geometries or plasma conditions, or the maximum electric field that can be supported across a rotating plasma. However, it is easy to demonstrate on an abstract plane that the hydromagnetic capacitor opens a new range of possibilities in fast-discharge work.

It is often stated that the amount of capacitor energy that can be delivered to a load in a given time interval is limited by the attainable dielectric constant of the capacitor. This is readily seen in the case of a one-dimensional transmission line of uniform K. Suppose that breakdown problems limit the tolerable electric field to an E_{max} that is independent of K. The maximum energy density and discharge velocity in the transmission line are

$$u_e = K (E_{max}^2 / 8\pi) \qquad (34)$$

and

$$v_d = c/\sqrt{K} \quad . \tag{6}$$

The maximum energy that can be delivered in a time τ to a load of cross section A is then given by

$$U = \sqrt{K}\,(A\, c\, \tau\, E_{max}^2 / 8\pi) \quad . \tag{35}$$

It is plain from Eq. (35) that U can be raised arbitrarily with K, until such considerations as mechanical pressure become significant. Even then no firm upper limit is encountered, since it has been shown that force-free coils permit magnetic energy densities far in excess of what is tolerable from the point of view of the strength of materials.[2]

The one-dimensional transmission line is a rather special case of a capacitor. In general one must consider the possibility of two or even three-dimensional complexes of conductor and dielectric. The question of the optimum dielectric constant in each case depends very much on topology and on various technical considerations. One of the few abstractions that can be made is that all geometries must reduce to the case of the one-dimensional transmission line in the limit of very short discharge times. The simple example of Fig. 11 will make this clear. Consider a capacitor of two infinite parallel plates separated by a medium of dielectric constant K. Through this sandwich there is a cylindrical incision of radius a. A cylindrical load is connected across the plates. During the discharge time τ, energy can come to the load only from within a distance $\lambda = v_d \tau$. Assuming unit spacing for the plates, one may write, for the upper limit of discharge energy delivered in time τ,

$$U = (K E_{max}^2 /8)\ [(\lambda + a)^2 - a^2]$$

$$= (c\, \tau\, E_{max}^2 /8)\ (c\, \tau + 2a\sqrt{K}). \tag{36}$$

As long as one has $c\,\tau \gg 2a\sqrt{K}$ it matters little whether K equals one or a million. This will for instance be true for τ = 1 μsec, a = 1 cm. On the other hand, for τ = 0.1 μsec, a = 10 cm, it is quite practical to have $2a\sqrt{K} \gg c\,\tau$. Under these conditions Eq. (36) can be reduced to the expression for the one-dimensional case, and the choice $K = 10^6$ permits almost ten times as much discharge energy as $K \ll 10^4$. It is seen that very large

dielectric constants are most advantageous in the limit $v_d \tau \leq a$, where the size of the high-K capacitor becomes comparable to or smaller than that of its load.

ACKNOWLEDGMENTS

The authors wish to thank Dr. Chester M. Van Atta for his constant support of this investigation, and gratefully acknowledge help by many members of the UCRL Sherwood research group. Particularly mentioned should be Mr. Elliot B. Hewitt for assistance in the measurements, Dr. John M. Stone, who performed the spectroscopic work, Dr. John Ise, Jr., who participated in some of the experiments, and Drs. Stirling A. Colgate and Allan N. Kaufman, who made valuable comments in discussions.

REFERENCES

1. Anderson, Baker, Colgate, Ise, and Pyle, Phys. Rev. 110, 1375 (1958).
2. Furth, Levine, and Waniek, Rev. Sci. Instr. 28, 949 (1957).
3. L. Spitzer, Physics of Fully Ionized Gases, (Interscience, London, 1956) p. 35.
4. Conrad L. Longmire, (LASL) private communication.
5. H. C. Early and W. G. Dow, Phys. Rev. 79, 186 (1950).
6. Allan N. Kaufman, (UCRL) private communication.
7. Anderson, Baker, Bratenahl, Furth, Ise, Kunkel, and Stone, The Homopolar Device, UCRL-8062, Dec. 1957.
8. H. C. Early and R. C. Walker, Transactions of the EIEE, Part I, vol. 31 p. 320 (1957).

FIGURE CAPTIONS

Fig. 1. Ion and electron trajectories in magnetic field crossed by electric field which slowly approaches its final value.

Fig. 2a. Cutaway view of hydromagnetic capacitor.

Fig. 2b. Equivalent coaxial capacitor.

Fig. 3. Observed current and voltage oscillograms.

Fig. 4. Calculated current and voltage in case of negligible leakage.

Fig. 5. Equivalent circuit of hydromagnetic capacitor experiment.

Fig. 6. Oscillogram of current and voltage with "crowbar" signal.

Figs. 7a and 7b. Superposition of observed crowbar signals.

Fig. 8. Analysis of Fig. 7a.

Fig. 9. Spectrum in normal and reversed magnetic field showing Doppler shift of the 3889 He line and of some strong lines of impurity ions.

Fig. 10. Oscillograms including spin loop and total light output signals.

Fig. 11. Capacitor as two-dimensional transmission line feeding into concentrated load.

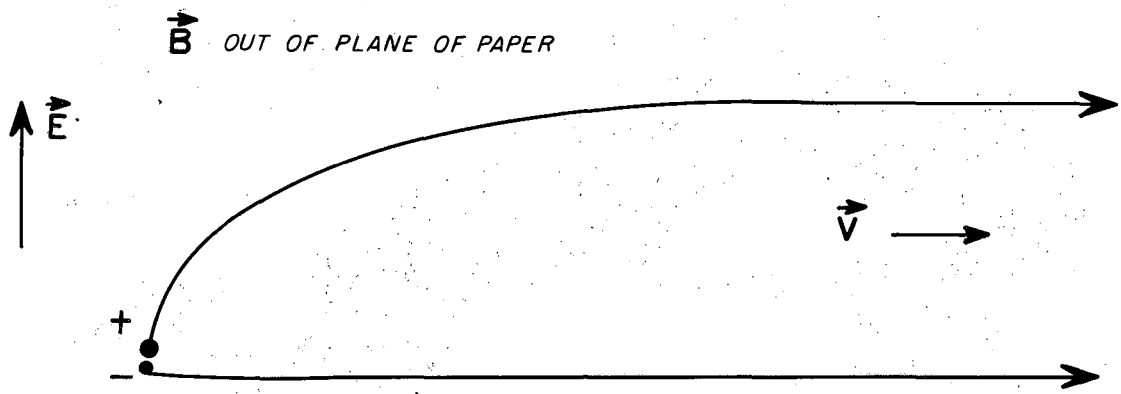

MU-15435

Fig. 1.

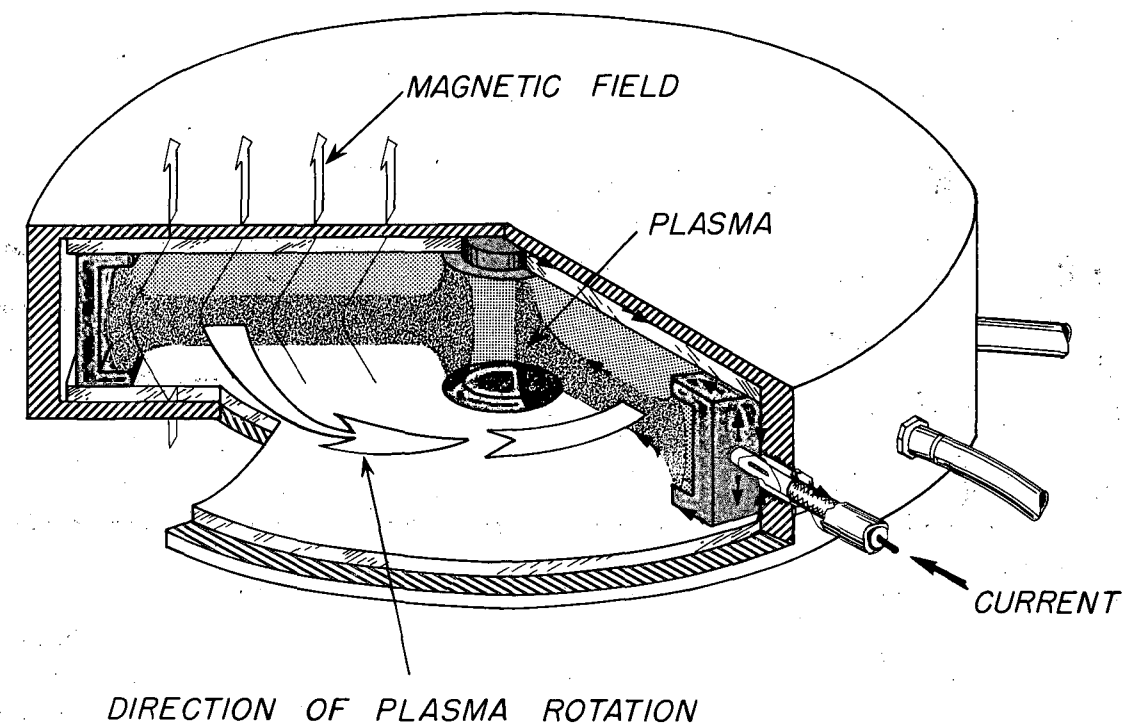
MAGNETIC FIELD
PLASMA
CURRENT
DIRECTION OF PLASMA ROTATION
MU-15433

Fig. 2a.

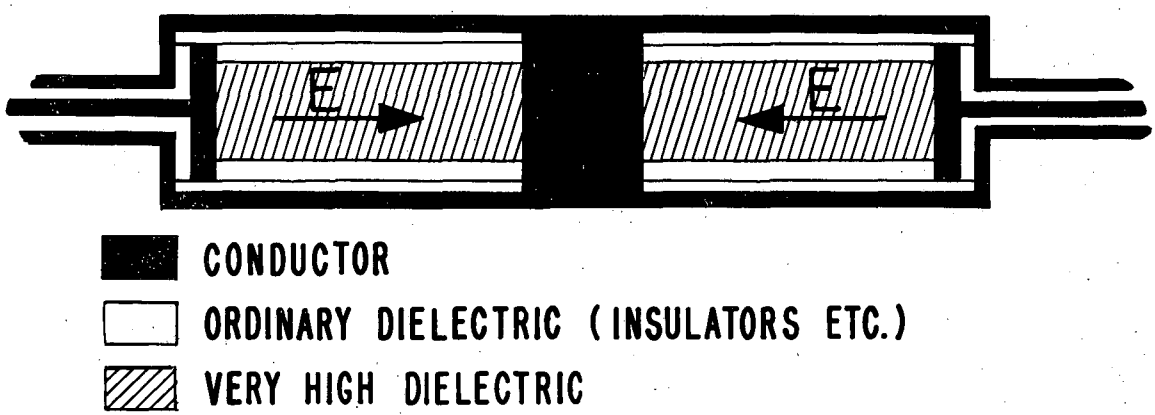

MU-15434

Fig. 2b.

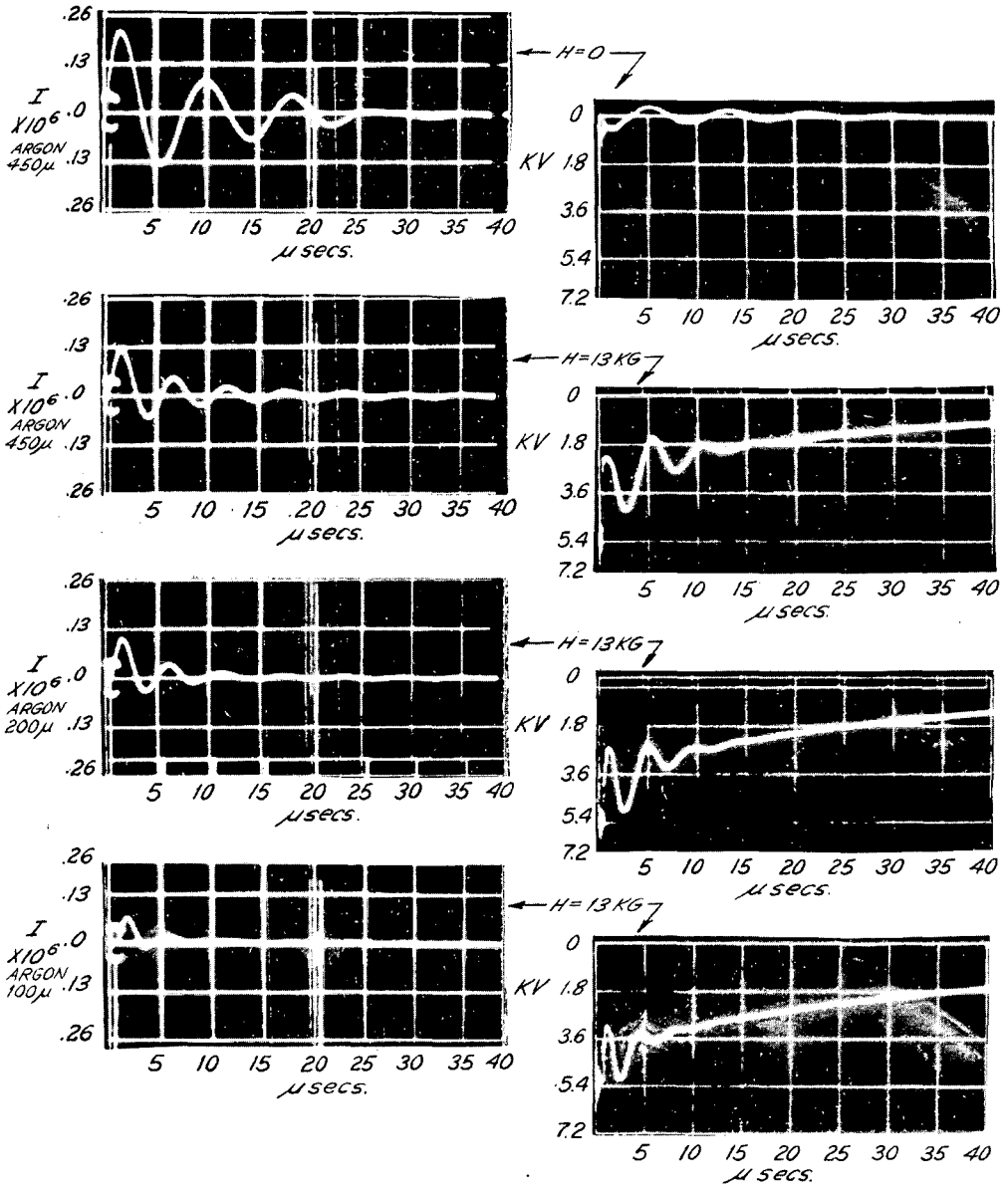
.26
.13
I
X10^6 .0
ARGON
450μ .13
.26
5 10 15 20 25 30 35 40
μ secs.
H=0
0
KV 1.8
3.6
5.4
7.2
5 10 15 20 25 30 35 40
μ secs.
.26
.13
I
X10^6 .0
ARGON
450μ .13
.26
5 10 15 20 25 30 35 40
μ secs.
H=13KG
0
KV 1.8
3.6
5.4
7.2
5 10 15 20 25 30 35 40
μ secs.
.26
.13
I
X10^6 .0
ARGON
200μ .13
.26
5 10 15 20 25 30 35 40
μ secs.
H=13KG
0
KV 1.8
3.6
5.4
7.2
5 10 15 20 25 30 35 40
μ secs.
.26
.13
I
X10^6 .0
ARGON
100μ .13
.26
5 10 15 20 25 30 35 40
μ secs.
H=13KG
0
KV 1.8
3.6
5.4
7.2
5 10 15 20 25 30 35 40
μ secs.

ZN-1961

Fig. 3.

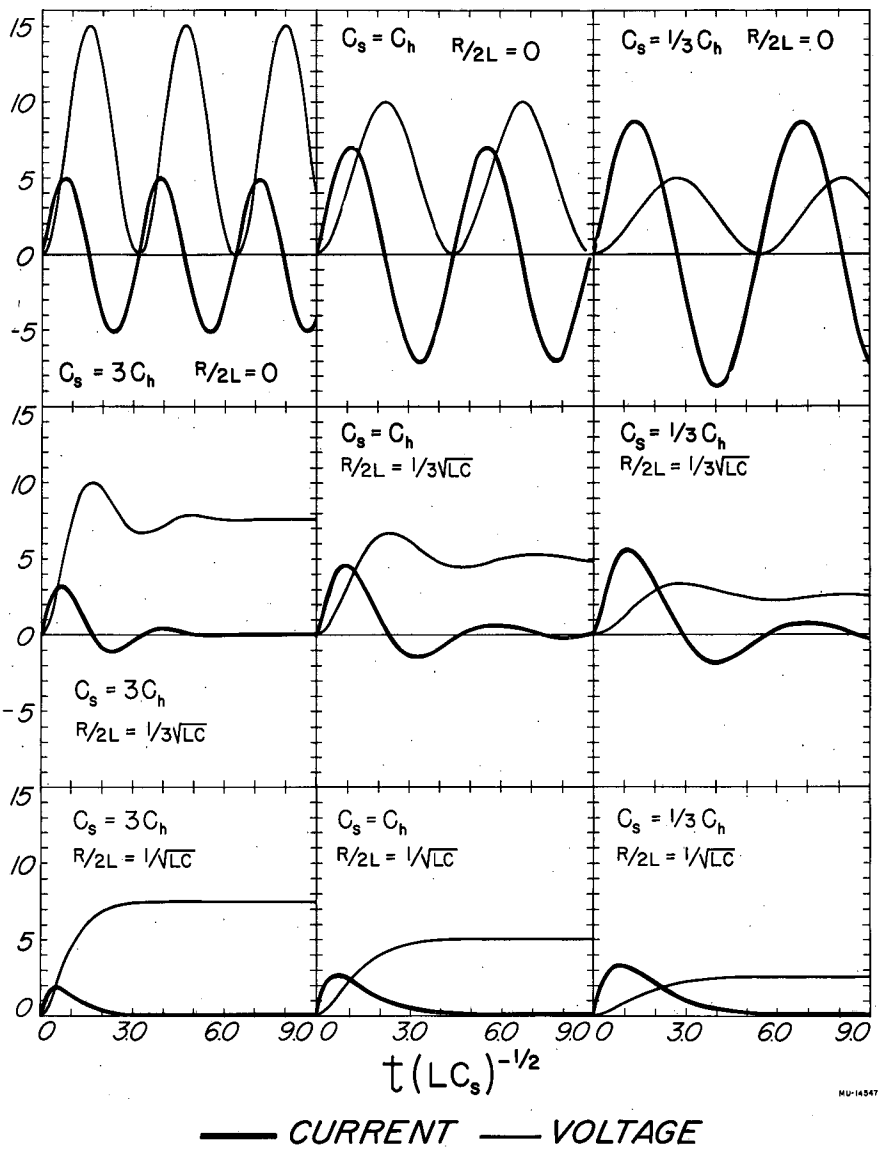
15
10
5
0
-5
$C_s = C_h$ R/2L = 0
$C_s = 1/3\,C_h$ R/2L = 0
$C_s = 3C_h$ R/2L = 0
$C_s = C_h$ R/2L = $1/3\sqrt{LC}$
$C_s = 1/3\,C_h$ R/2L = $1/3\sqrt{LC}$
$C_s = 3C_h$ R/2L = $1/3\sqrt{LC}$
$C_s = 3C_h$ R/2L = $1/\sqrt{LC}$
$C_s = C_h$ R/2L = $1/\sqrt{LC}$
$C_s = 1/3\,C_h$ R/2L = $1/\sqrt{LC}$
0 3.0 6.0 9.0
$t(LC_s)^{-1/2}$
MU-14547
CURRENT VOLTAGE

Fig. 4.

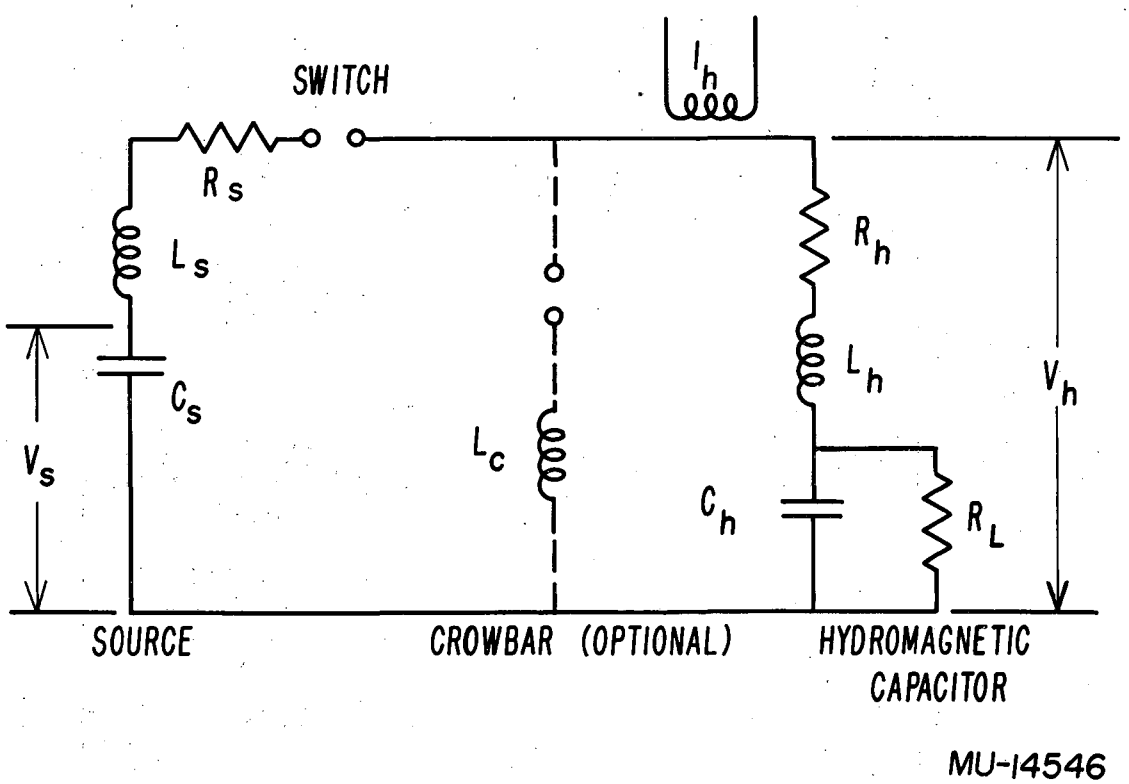
SWITCH
I_h
R_s
L_s
C_s
V_s
L_c
R_h
L_h
C_h
R_L
V_h
SOURCE
CROWBAR (OPTIONAL)
HYDROMAGNETIC CAPACITOR
MU-14546

Fig. 5.

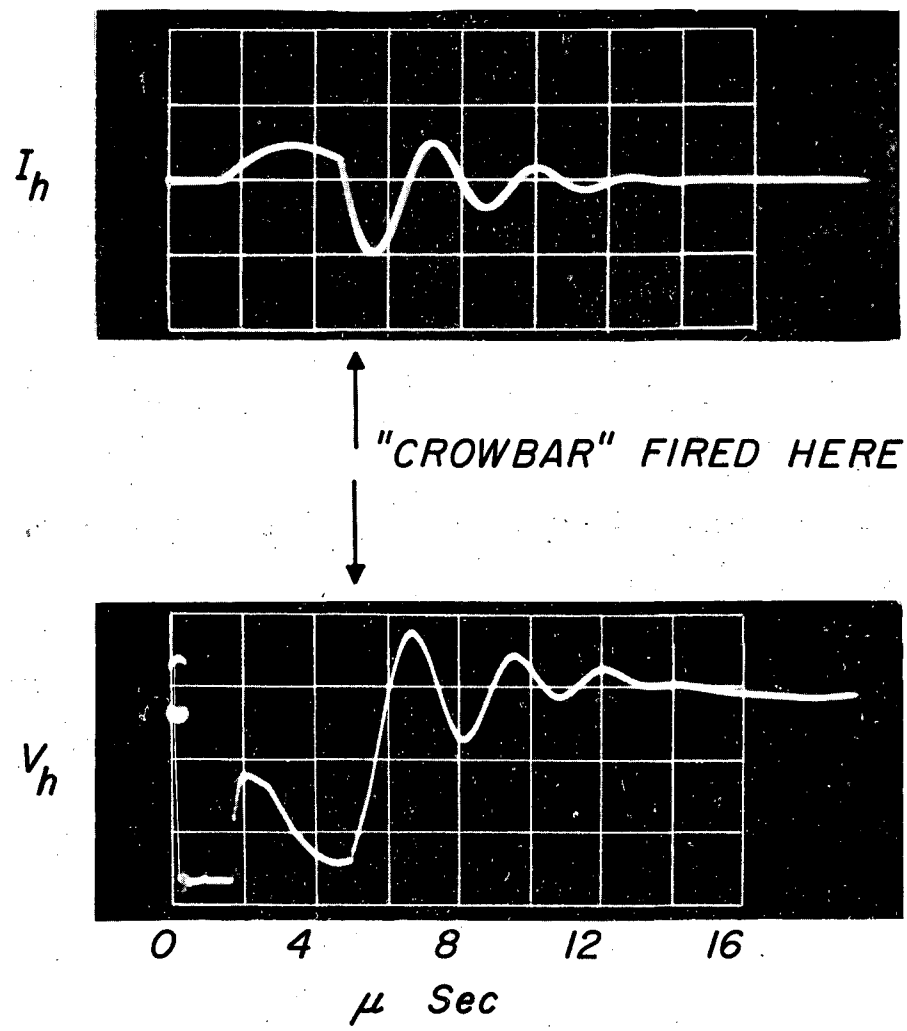
I_h
"CROWBAR" FIRED HERE
V_h
0
4
8
12
16
μ Sec
15 KG
400μ ARGON
6 KV
ZN-1962

Fig. 6.

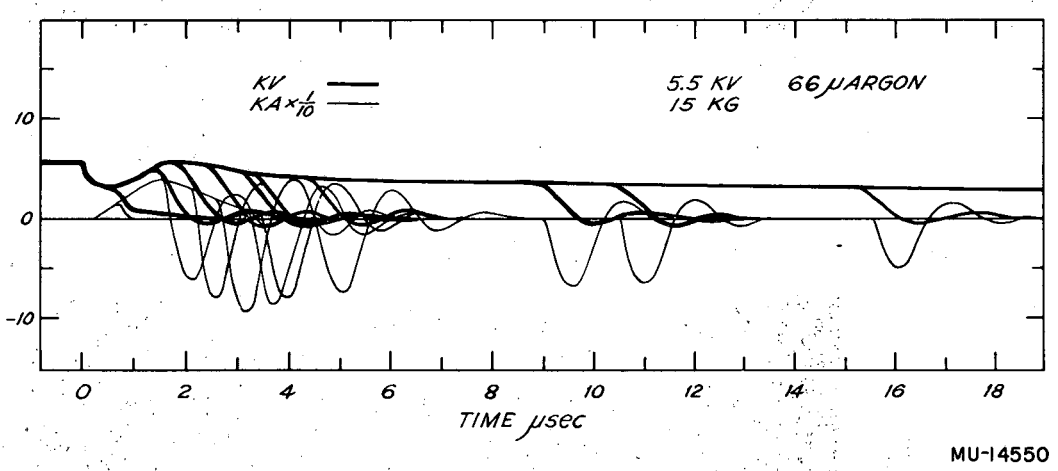
(a)
KV
KA × 1/10
5.5 KV
15 KG
66 μ ARGON
10
0
-10
0
2
4
6
8
10
12
14
16
18
TIME μsec
MU-14550

Fig. 7a.

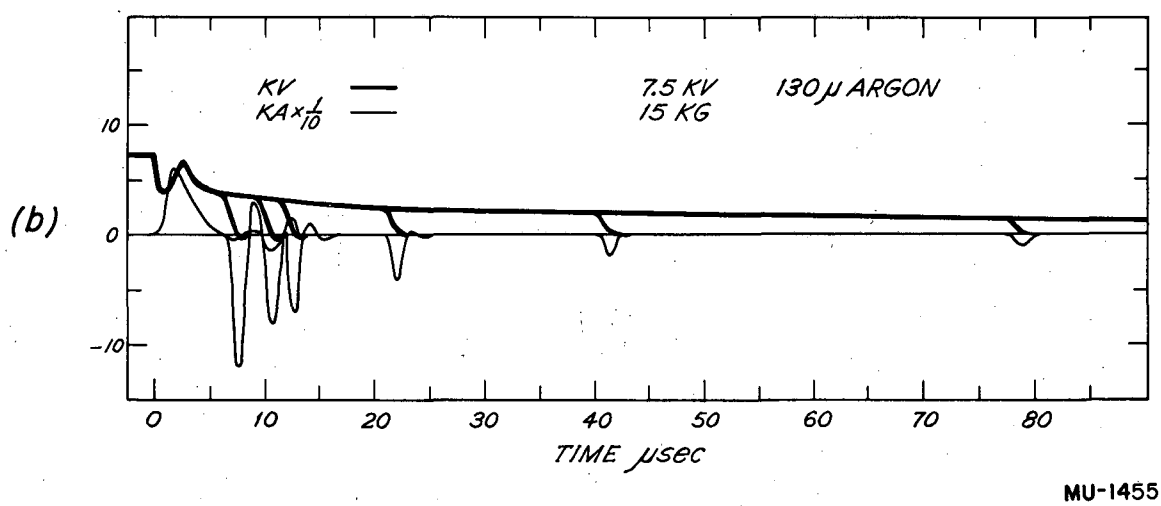
(b)
KV
KA x 1/10
7.5 KV
15 KG
130 μ ARGON
10
0
-10
0
10
20
30
40
50
60
70
80
TIME μsec
MU-14551

Fig. 7b.

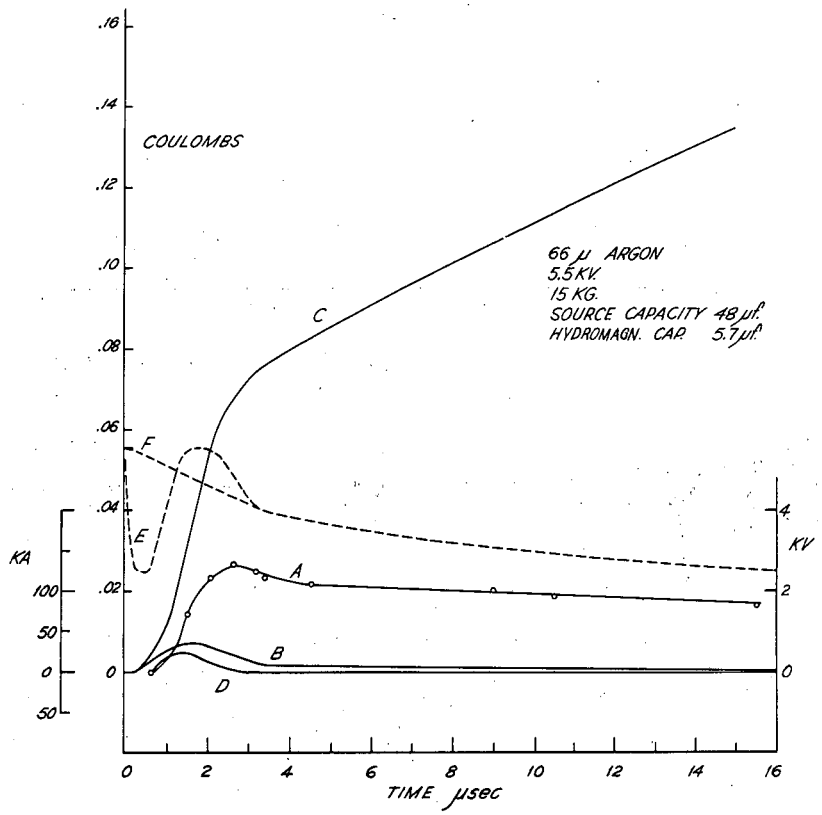

CROWBAR CHARGE - CURVE A
CURRENT FROM SOURCE - CURVE B
CHARGE FROM SOURCE - CURVE C
HYDROMAGN. CHARGE CURRENT - CURVE D
HYDROMAGN. VOLTAGE - CURVE E
SOURCE VOLTAGE - CURVE F

MU-14553

Fig. 8.

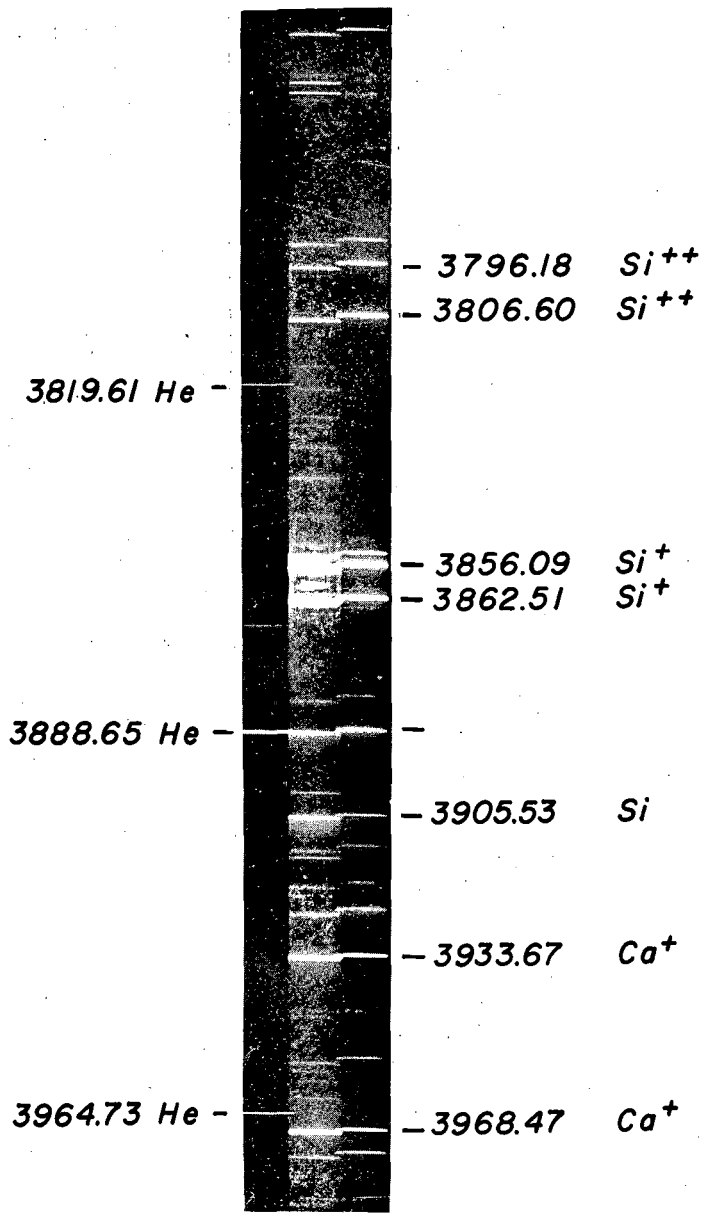
3796.18 Si++
3806.60 Si++
3819.61 He
3856.09 Si+
3862.51 Si+
3888.65 He
3905.53 Si
3933.67 Ca+
3964.73 He
3968.47 Ca+
ZN-1963

Fig. 9.

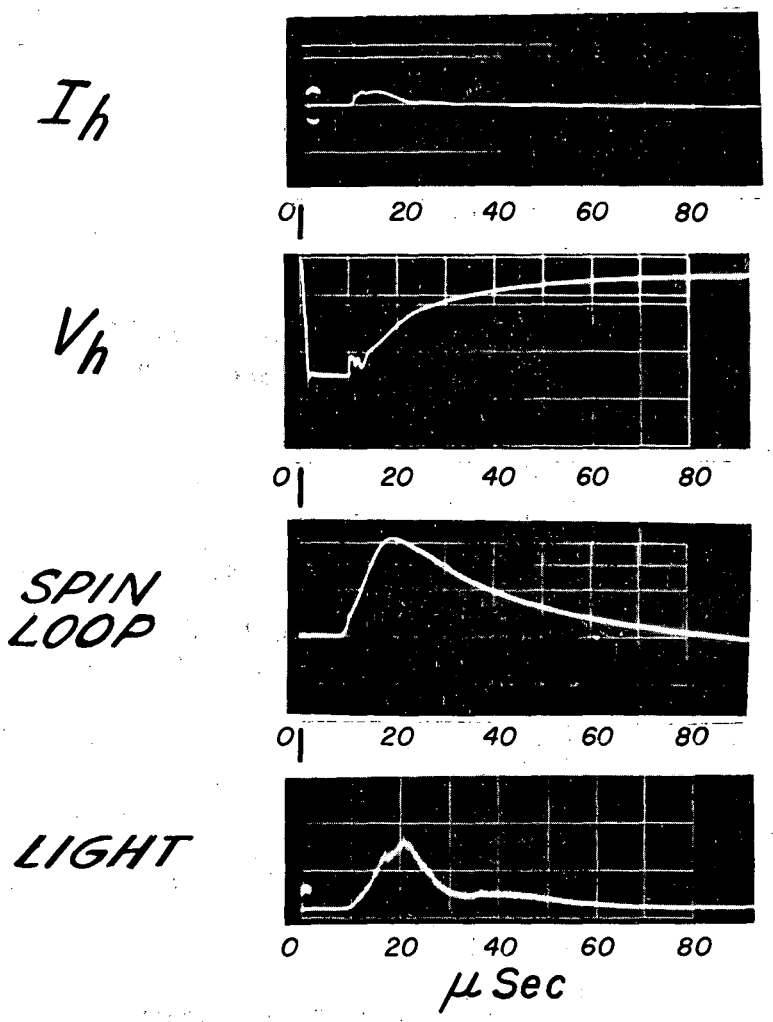

ZN-1964

Fig. 10.

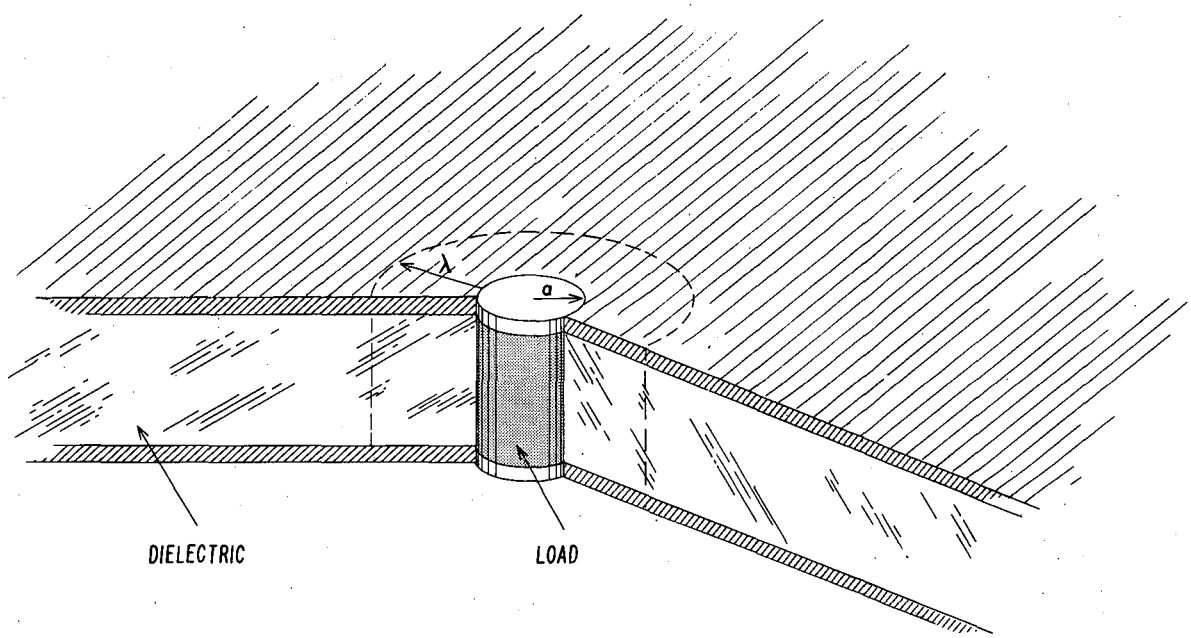

Fig. 11.